

RESEARCH

Open Access



# Innovations in radiotherapy for tongue squamous cell carcinoma

Songling Hu<sup>1,2,3\*</sup>, Xiaofei Li<sup>1,2,3\*</sup>, Bin Yang<sup>1,2</sup>, Tian Yu<sup>1,2</sup>, Fangyu Yi<sup>1,2</sup>, Xiurong Qin<sup>1,2</sup>, Cong Chen<sup>1,2</sup>, Can Wang<sup>1,2</sup>, Xin Yu<sup>1,2</sup> and Jing Zhu<sup>1,2\*</sup>

## Abstract

Radiotherapy sensitivity is associated with the prognosis of patients with tongue squamous cell carcinoma (TSCC). In the present study, we proposed to explore the specific mechanism of interventional radiology (IR) therapy for TSCC in vitro and in vivo. TSCC cells were treated with 6 Gy IR and tumor bearing mice were treated with 20 Gy × 1 IR. DIA quantitative proteomics along with bioinformatics analysis were conducted in TSCC cells to investigate differential proteins related to IR and relation of which involved in TMEM147 and SPHK1 was confirmed by immunoprecipitation. Cell proliferation, apoptosis, autophagy & autophagy flux along with calcium signaling pathway detection were performed in vitro and in vivo. Our results showed that IR induced increasing calcium levels accompanied by up-regulated TMEM147 and down-regulated SPHK1 along with enhancing autophagy together with apoptosis. The effect of calcium overloading induced by IR on autophagy and apoptosis was dependent on increasing TMEM147 and decreasing SPHK1. However, IR-induced autophagy and apoptosis tended to be independent of only increasing calcium levels when down-regulating TMEM147 or up-regulating SPHK1 expression in vitro and in vivo. Our study suggested that calcium-mediated TMEM147/SPHK1 may promote autophagy and apoptosis to improve radiotherapy sensitivity in TSCC.

**Keywords** Tongue squamous cell carcinoma, Interventional radiology, Calcium, TMEM147, SPHK1, Autophagy

## Introduction

Tongue squamous cell carcinoma (TSCC) is one of the most common cancers occurring in oral cavity cancer [1, 2]. The incidence of TSCC is reported to be increasing among people < 45 years in some countries according to

the data derived from patients age ≥ 20 years diagnosed with tongue cancer between April 2008 and January 2019 extracted from Diagnosis Procedure Combination database [2, 3]. As noted in a previous study involving 346 patients with TSCC based on Hospital Cancer Registry System Data and Mortality Information from 2007 to 2009, 71.1% were advanced staging at the time of diagnosis and presented a high mortality rate (72.5%) [4]. TSCC is not obvious and easy to miss the opportunity for early diagnosis when in the advanced stage presently [5]. Surgery accompanied by another treatment modality, such as chemotherapy and interventional radiology (IR), remains the common treatment approach for TSCC which affects 5 year specific survival of TSCC patients at present. Therefore, it is necessary to explore the molecular mechanisms affecting the efficacy of TSCC to improve the prognosis of patients presently.

\*Correspondence:

Songling Hu  
18111140002@fudan.edu.cn  
Xiaofei Li  
Jing Zhu  
zhujing1101@163.com

<sup>1</sup> Department of Preventive Dentistry, Shanghai Stomatological Hospital & School of Stomatology, Fudan University, 1258 Fuxing Middle Road, Shanghai 200001, China

<sup>2</sup> Shanghai Key Laboratory of Craniomaxillofacial Development and Diseases, Fudan University, Shanghai 200001, China

<sup>3</sup> Institute of Radiation Medicine, Shanghai Medical College, Fudan University, Shanghai 200032, China



© The Author(s) 2024. **Open Access** This article is licensed under a Creative Commons Attribution-NonCommercial-NoDerivatives 4.0 International License, which permits any non-commercial use, sharing, distribution and reproduction in any medium or format, as long as you give appropriate credit to the original author(s) and the source, provide a link to the Creative Commons licence, and indicate if you modified the licensed material. You do not have permission under this licence to share adapted material derived from this article or parts of it. The images or other third party material in this article are included in the article's Creative Commons licence, unless indicated otherwise in a credit line to the material. If material is not included in the article's Creative Commons licence and your intended use is not permitted by statutory regulation or exceeds the permitted use, you will need to obtain permission directly from the copyright holder. To view a copy of this licence, visit <http://creativecommons.org/licenses/by-nc-nd/4.0/>.

IR employs image-guided techniques to perform minimally invasive procedures for diagnosis and treatment which has evolved tremendously since the early 20th century and is now a distinct clinical discipline [6]. IR approaches are being used in oncology for local diagnosis and treatment with minimally invasive therapeutic and palliative options. Tumor sensitivity to IR associated with prognosis of many patients with cancers including TSCC [7, 8]. Radiation therapy as well as targeted delivery of chemotherapy are being developed as alternatives when surgery is not feasible for cancer patients [9]. However, radiotherapy resistance is not conducive to the prognosis of cancer patients. Resistance to radiotherapy remains one of major clinical challenges which highlights the need to identify predictive markers for improving radiotherapy resistance. It was reported in recently studies that green nanomaterials such as green-synthesized silver nanoparticles from biological sources may be potential strategies to sensitize cancer cells to radiotherapy due to their low toxicity [10] besides their activities of antioxidant, antipathogenic, anticholinesterase [11] as well as antimicrobial and cytotoxic activities [12]. However, the stability and applicability in radiotherapy sensitivity to TSCC of nanomaterials remains to be further explored at present. Moreover, programmed cell death, such as autophagy and apoptosis correlate with IR therapy for cancer. The effect of Iodine-125 seed radiation on esophageal squamous cell carcinoma was enhanced by inhibition of endoplasmic reticulum stress-mediated autophagy [13]. Promoting apoptosis is helpful to sensitize oral tongue squamous cell carcinoma cells to radiation [14]. In general, regulating autophagy and apoptosis of cancer cells would be conducive to improving the prognosis of patients with TSCC which is involved in our study.

In the present study, we proposed to explore the specific mechanism of IR therapy for TSCC in vitro and in vivo. Based on IR treatment for TSCC cells and tumor bearing mice, DIA quantitative proteomics along with bioinformatics analysis, calcium detection, immunoprecipitation and autophagy flux, etc., Relation of differential proteins such as TMEM147 and SPHK1, calcium signaling pathway, autophagy and apoptosis with IR sensitivity

was investigated in our study, result of which would be beneficial to elucidate mechanism of IR therapy for TSCC to improve the prognosis of patients.

## Materials and methods

### Materials

Thapsigargin (T9033) was purchased from Sigma-Aldrich (USA). Antibodies of TMEM147(ab97624, Abcam), SPHK1(ab302714, Abcam), P62(ab109012, Abcam), mTOR(2983T), p-mTOR(5536T), AMPK(2532), pAMPK(2535T), LC3II/I(12741T), Caspase 3(14220T) and Cleaved Caspase 3(9664T) were supplied by Cell Signaling Technology.

Vectors of down-expression TMEM147(shTM147) and SPHK1(sh SPHK1) as well as over-expression TMEM147(TM147-OE), SPHK1(SPHK1-OE) and negative control (shNC and OE-NC) were obtained from Genechem, Shanghai, China .

### Cells and cell culture

Cell lines of CAL27, HSC3 and SAS were supplied by Guangzhou Cellcook Biotech Co.Ltd. CAL27 and HSC3 were cultured in DMEM medium (11095080, Gibco) supplemented with 10% FBS (10091148, Gibco) and SAS cells were cultured in DMEM/F12 (10566016, Gibco) supplemented with 10% FBS. All the cells were incubated in an incubator with 5% CO<sub>2</sub> at 37 °C.

## Methods

### CCK8 assay

The 10<sup>4</sup>cells/well were planted in a 96-well plate. After interventional radiology (IR) treatment with 0–8 Gy according to previous studies [15, 16], 10 μL/well CCK8 was added to the cells and then incubated at 37 °C for 2 h. Absorbance value at 450 nm was obtained from a microplate reader. Cell survival may be calculated from the value.

### Apoptosis was detected on a flow cytometry

The cells of CAL27, HSC3 and SAS transfected with/without si(OE)NC or siTM147/SPHK1-OE along with/without IR were incubated with PI/APC according to the instructions of Annexin V-APC apoptosis detection kit

(See figure on next page.)

**Fig. 1** Genes associated with IR sensitivity of cells in tongue squamous cell carcinoma screening. **A** The viability of CAL27, HSC3 and SAS cells treated with 0–8 Gy was assayed by CCK8. n = 3. ns means the difference is not significant. **B** Apoptosis of CAL27, HSC3 and SAS cells treated with 6 Gy was detected by flow cytometry. **C** Apoptosis rate was analyzed. n = 3, \*\*\*P < 0.001. **D** Venn diagram of differential proteins in IR treated CAL27, HSC3 and SAS cells compared with control. **E** Five distinct proteins in IR treated CAL27, HSC3 and SAS cells compared with control. **F** Heat map of TMEM147/SPHK1 in IR treated SAS cells compared with control. **G** Bubble diagram of differential proteins of IR treated CAL27, HSC3 and SAS cells compared with control enrichment in Kegg pathway. **H** Histogram of differential proteins of IR treated CAL27, HSC3 and SAS cells compared with control enrichment in Kegg pathway

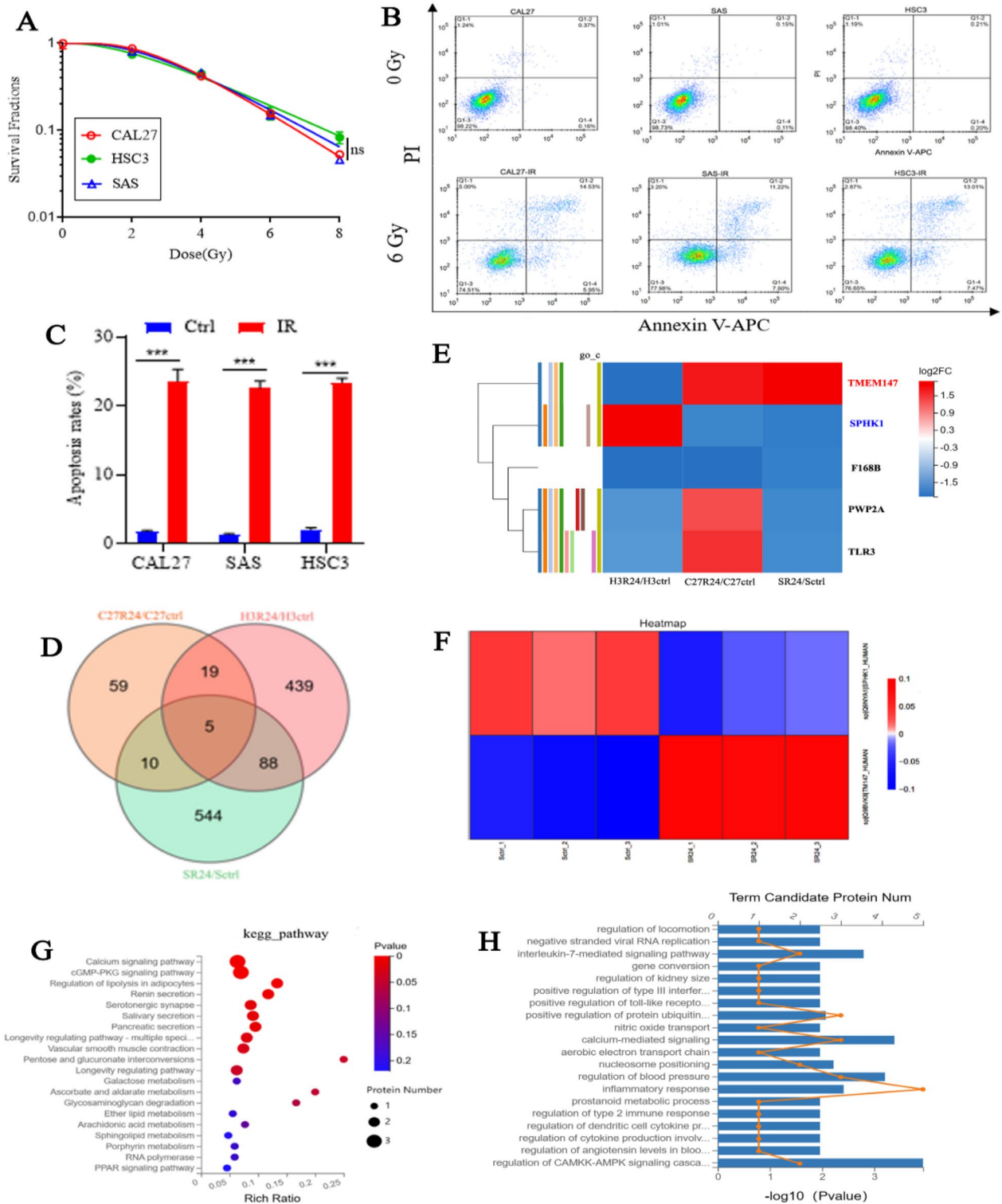


**Fig. 1** (See legend on previous page.)

(Share-bio, SB-Y6026, 647-Annexin V/PI). After preprocessing based on the operation manual of the kit, apoptosis of cells was analyzed on a flow cytometry.

**DIA quantitative proteomics analysis**

Total proteins of CAL27, SAS and HSC-3 cells were extracted and their concentrations were detected with

BCA assay (Beyotime Biotechnology, P0012). The identification of proteins by DIA depends on a data dependent acquisition (DDA) library. MaxQuant was then used to complete library search identification to obtain all detectable non-redundant high-quality MS/MS spectra information, which is used as a subsequent data independent acquisition (DIA) quantitative spectra library. Then IBT quantitative analysis was conducted to screen out significantly differential proteins that we were more concerned about from the quantitative results. Finally, GO, Pathway, KOG and other functional annotations and GO, KOG and Pathway enrichment analysis of differential proteins were further conducted.

### Experiments of tumor-bearing animals

All the animal experiments were performed according to the ethics committee on animal experiments of Fudan University. 6–8 weeks old male BALB/c nude mice, weight  $20 \pm 2$  g, were purchased from Shanghai Shengchang Bio-Tech Pty Ltd (SCxK(Shanghai)2021-0002) in our study. After one week of adaptive feeding,  $10^6$  cells/mouse in 100 $\mu$ L PBS were subcutaneously inoculated into the armpit of the right forelimb of nude mice. The tumor bearing mice were treated with 20 Gy  $\times$  1 IR on day 9 after tumor cells inoculation according to previous studies [17, 18]. Tumor volume was recorded every two days. The tumor growth curves were plotted based on the tumor volume.

### Calcium levels assay

$0.5 \times 10^4$  cells/well were planted in a 12-well plate, after treated with/without IR and/or Thapsigargin as well as transfected with shTM147, shSPHK1, TM147-OE, SPHK1-OE, shNC and OE-NC, Calcium ion fluorescent probe Fluo-4 Calcium Assay Kit (Beyotime Biotechnology, Shanghai, S1061S) was added to the cells, images of cells with green fluorescence were obtained to indicate calcium in an hour.

### Western blotting

The total protein of cells and tissue was obtained using PMSF (100mM) at first followed by protein concentration detection using a BCA kit (Beyotime Biotechnology

Co., Shanghai, China, P0010) according to the instruction. The proteins were isolated by SDS-PAGE, and then transferred to PVDF membrane (0.2  $\mu$ m, Merck Millipore Ltd, USA, 03010040001) and incubated with the primary antibodies of TMEM147 (1:500), SPHK1 (1:500), mTOR (1:500), p-mTOR (1:200), AMPK (1:500), pAMPK (1:200), P62 (1:500), LC3II/I(1:500), Caspase 3 (1:500) and Cleaved Caspase 3 (1:200) followed by incubation with the corresponding secondary antibody. After being immunoblot stained by ECL staining system, images of blots were acquired under a chemiluminescence imager. Grayscale values of blots were analyzed using ImageJ software.

### Autophagy was observed by transmission electron microscopy

The cells were collected and fixed in 1% osmium acid prepared with 0.1 M phosphate buffer PB (PH7.4) at room temperature in the dark for 2 h. Then the cells were sequentially added 30% –50% –70% –80% –95% –100% –100% alcohol for 20 min each time, and 100% acetone twice for 15 min each time. Penetration embedding was performed as follows: acetone and 812 embedding agents with the rate 1:1 at 37 °C for 2 h followed by 1:2 overnight penetration, pure 812 embedding agent at 37 °C for 5 h. Pour pure 812 embedding agent into the embedding plate, insert the sample into the embedding plate, and bake overnight at 37 °C. 60–80 nm ultra-thin sections were made and 150 mesh film copper mesh is used for fishing. Copper mesh was dyed in a 2% uranyl acetate saturated alcohol solution in the dark for 8 min and 2.6% lead citrate solution was utilized to avoid carbon dioxide staining for 8 min. After washing, the slices of the copper mesh were placed in a copper mesh box to dry overnight at room temperature. The autophagosomes were observed under a transmission electron microscope, and images were acquired and analyzed by HITACHI HT 7800 instrument (Japan).

### Autophagy flux assay

Autophagy was examined by analyzing the formation of fluorescent puncta of autophagosomes in the cells

(See figure on next page.)

**Fig. 2** Calcium-mediated mTOR/AMPK signaling involved in IR sensitivity of cells in tongue squamous cell carcinoma. **A** Tumor growth in mice inoculated subcutaneously with CAL27 and SAS treated with/without IR and Thapsigargin. **B** Tumor growth curve of mice inoculated subcutaneously with CAL27 was plotted.  $n = 5$ , \* $P < 0.05$  **C** Tumor growth curve of mice inoculated subcutaneously with SAS was plotted.  $n = 5$ , \* $P < 0.05$  **D** Calcium levels image of CAL27 and SAS cells treated with/without IR and Thapsigargin. **E** Calcium levels of CAL27 and SAS cells treated with/without IR and Thapsigargin was analyzed.  $n = 3$ , \* $P < 0.05$ , \*\* $P < 0.01$ . **F** The protein expression of (p) mTOR, (p) AMPK, TMEM147 and SPHK1 in CAL27 cells treated with/without IR and Thapsigargin was detected using western blotting. **G** Histogram of protein expression of (p) mTOR, (p) AMPK, TMEM147 and SPHK1 in CAL27 cells treated with/without IR and Thapsigargin. **H** The protein expression of (p) mTOR, (p) AMPK, TMEM147 and SPHK1 in SAS cells treated with/without IR and Thapsigargin was detected using western blotting. **I** Histogram of protein expression of (p) mTOR, (p) AMPK, TMEM147 and SPHK1 in SAS cells treated with/without IR and Thapsigargin.  $n = 3$ , \* $P < 0.05$ , \*\* $P < 0.01$

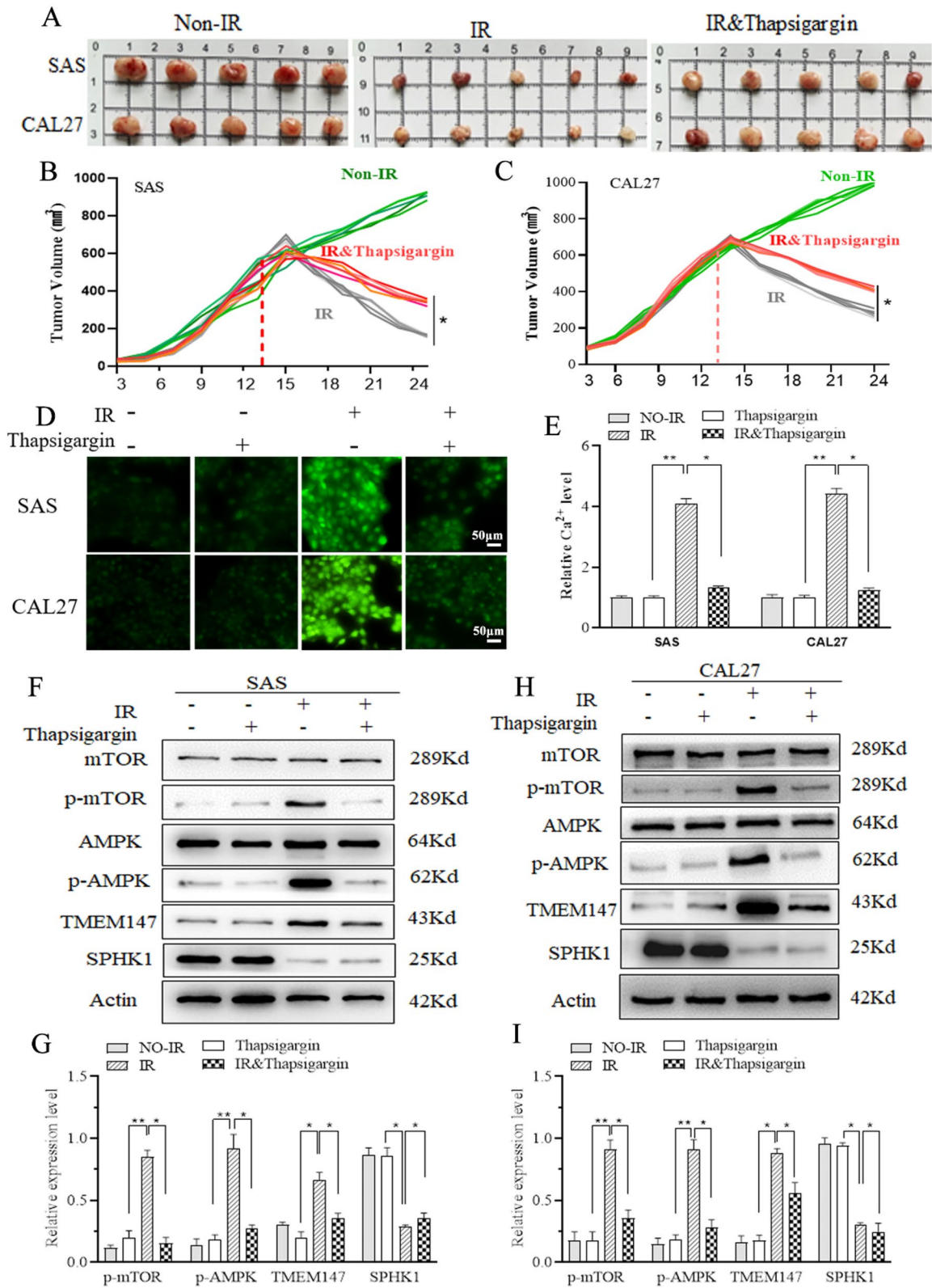


**Fig. 2** (See legend on previous page.)

transfected with mRFP-GFP-LC3-tagged adenovirus (Hanbio Biotechnology Co., Shanghai, China). Briefly, cells were plated at a density of  $2 \times 10^5$  per well in 24-well plate and cultured overnight. After 2 h of transfection with the adenovirus (diluted in serum-free medium), the cells were cultured in fresh medium for 48 h then washed with pre-cooled PBS twice, fixed and stained with DAPI. The intracellular autophagy was observed with the high-content imaging system. When the fusion of autophagy and lysosome occurs, LC3-GFP fluorescence is quenched and only red fluorescence can be observed. After merging the red and green fluorescence images, yellow spots in the cell images symbolize the puncta of autophagosomes. For quantitative analyses, the numbers of yellow (autophagosomes) and red only puncta (autolysosomes) and ratio of autolysosomes to autophagosomes were quantified per OSCC cell from random fields in three independent experiments (totally  $n = 50$  cells).

#### Clone formation

$10^4$  cells /well was planted in a 6-well plate pre-covered with agar gel. The cells treated with/without IR and/or Thapsigargin as well as transfected with shTM147, shSPHK1, TM147-OE, SPHK1-OE, shNC and OE-NC were allowed to grow for 2 weeks. Then 1 ml crystal violet solution was added to the cells. After washing using PBS three times, images of cells were taken and the number of clones was analyzed.

#### Tunnel staining

The slices of tumor tissue were deparaffinized and dehydrated in xylene and in gradient ethanol of 95%, 90%, 80%, and 70%, respectively. After washing, antigen retrieval was performed with proteinase K in PBS (pH 7.4). Permeability solution (0.1% Triton) was added to the sections for permeabilization. Equilibrium at room temperature was performed, then reaction solution including TDT enzyme and dUTP was added to the sections and incubated at 37°C for 2 h. DAPI was used to counterstain nucleus. The sections were observed under a fluorescence microscope and images were collected by Panoramic MIDI instrument (3DHISTECH, Ltd. Hungary). DAPI ultraviolet excitation wavelength was 330–380 nm,

emission wavelength was 420 nm. CY3 excitation wavelength was 510–561 nm, emission wavelength was 590. The nuclei stained by DAPI are blue under the excitation of ultraviolet light, the Tunnel kit is labeled with CY3 fluorescein, and the positive apoptosis nuclei are red.

#### Immunofluorescence detection

The paraffin sections of tumor tissues were sequentially dewaxed to water in xylene, 85% alcohol and 75% alcohol first. After washing, antigen repair was performed in EDTA (PH9.0) antigen repair solution. The sections were incubated with BSA for blocking for 30 min. The first type of primary antibody of TMEM147 (1:200) was added to the sections and incubated overnight at 4°C in a wet box followed by incubation with the corresponding secondary antibody. After washing, antigen repair, and blocking similarly to the aforementioned methods, the secondary antibody of SPHK1 (1:100) was added to the sections followed by the corresponding secondary antibody (Cell Signaling technology, 4412 S) and incubated similarly.  $\gamma$ H2AX (1:200) immunofluorescence detection was similar to TMEM147. DAPI was used to stain nucleus (Beyotime Biotechnology Co., Shanghai, China, P0131). After sealing, slices were observed and images were collected under a fluorescence microscope. The nuclei stained by DAPI was blue, and positive expression is indicated by corresponding fluorescent labeled red or green light.

#### Statistical analysis of data

All measurement data are represented by mean  $\pm$  SD. The difference between two groups was analyzed using non paired t-test. The difference among three or more groups were analyzed using one-way ANOVA corrected with Bonferroni post hoc tests. The difference was considered significant when the *P* value was less to 0.05.

## Results

### TMEM147/SPHK1 associated with IR sensitivity of cells in tongue squamous cell carcinoma

To explore IR sensitivity markers in tongue squamous cell carcinoma, viability of tongue squamous cell carcinoma cell lines such as CAL27, HSC3 and SAS after

(See figure on next page.)

**Fig. 3** Relation of Calcium, autophagy and apoptosis with IR sensitivity of cells in tongue squamous cell carcinoma. **A** Autophagosomes were observed in SAS cells treated with/without IR and Thapsigargin using transmission electron microscope. **B** Autophagosomes were observed in CAL27 cells treated with/without IR and Thapsigargin using transmission electron microscope. The red arrows indicate the autophagosomes with bilayer structure. The blue arrows indicate the decreasing autophagy. **C** The protein expression of P62, LC3II/I and (Cleaved) Caspase 3 in CAL27 cells treated with/without IR and Thapsigargin was detected using western blotting. **D** The protein expression of P62, LC3II/I and (Cleaved) Caspase 3 in SAS cells treated with/without IR and Thapsigargin was detected using western blotting.  $n = 3$ , \* $P < 0.05$ , \*\* $P < 0.01$ . **E, F** Autophagy flux was observed in CAL27 and SAS cells treated with/without IR and Thapsigargin and transfected with GFAP/RFP fluorescent label LC3 expression vector

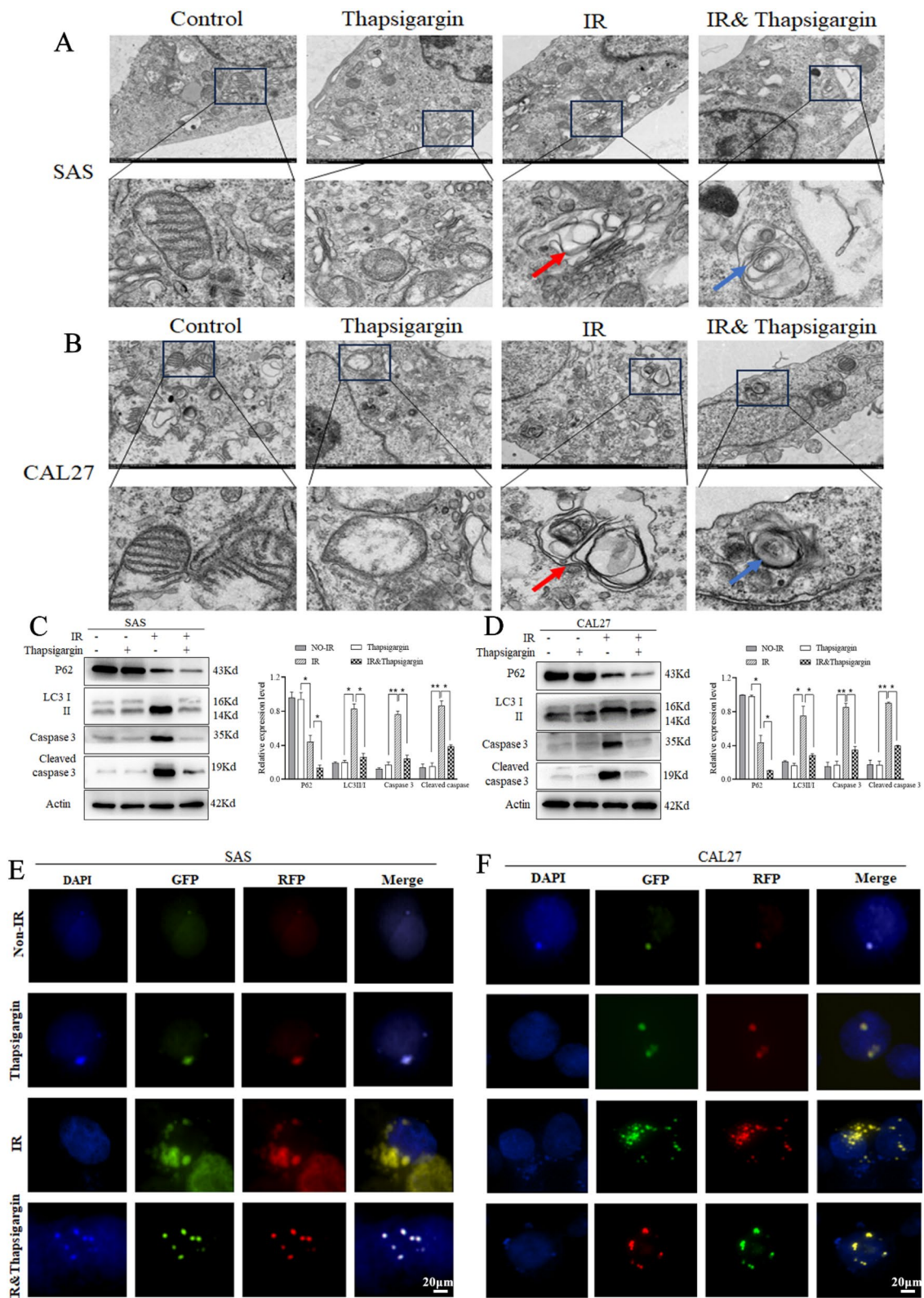


**Fig. 3** (See legend on previous page.)

treatment with IR at the dose of 0 to 8 Gy was detected firstly. Results showed in Fig. 1A that cell survival was decreased dose-dependently and the median inhibition rate dosed was about 6 Gy, which was therefore chosen for subsequent experiments. The apoptosis rate of CAL27, HSC3 and SAS treated with 6 Gy was significantly decreased compared with control cells (Fig. 1B, C). The differential proteins were then investigated in the three cell lines treated with 6 Gy and the corresponding control cells by DIA quantitative proteomics analysis. As indicated in Fig. 1D, five differential proteins including SPHK1, TMEM147, F158B, PWP2A and TLR3 were obtained in three cell lines (Fig. 1D, E). Further analysis results showed that TMEM147 expression was up-regulated while SPHK1 was down-regulated in both CAL27 and SAS cells, especially in SAS treated with IR compared with control cells (Fig. 1F). Results of enrichment pathways analysis of differential proteins demonstrated that calcium signaling pathway or calcium-mediated signaling and regulation of CAMKK-AMPK signaling cascade were involved (Fig. 1G, H).

#### Calcium-mediated AMPK/mTOR signaling involved in IR sensitivity of cells in tongue squamous cell carcinoma

The correlation of calcium-mediated AMPK signaling with IR sensitivity in tongue squamous cell carcinoma was explored in our study. The role of calcium in IR sensitivity in tumor-bearing mice was investigated, results of which were shown in Fig. 2A–C that IR suppressed tumor growth in mice subcutaneously inoculated with tumor cells of CAL27 and SAS significantly. Thapsigargin, a microsomal Ca<sup>2+</sup>-ATPase inhibitor, partially reversed the effect of IR on tumor growth. Results of calcium level detection showed that IR significantly induced calcium levels increasing in tongue squamous cell carcinoma cells which was attenuated by Thapsigargin (Fig. 1D, E). AMPK and mTOR signaling was next explored. It was showed in Fig. 2D, E that IR induced the expression of p-mTOR, p-AMPK increased accompanied with TMEM147 along with decreased SPHK1 expression. It was noting that Thapsigargin partially reversed

the effect of IR on the expression of p-mTOR, p-AMPK, TMEM147, SPHK1 complied with calcium levels.

#### Calcium-mediated autophagy and apoptosis associated with IR sensitivity of cells in tongue squamous cell carcinoma

AMPK and mTOR signaling is concerned in apoptosis and autophagy of tumor cells [19, 20]. Therefore, the role of calcium in the regulation of apoptosis and autophagy in relation to IR sensitivity of cells in tongue squamous cell carcinoma was in the following study. IR induced obvious autophagy of CAL27 and SAS compares with control cells. And there was no significant difference between Thapsigargin treated cells without IR and control cells (Fig. 3A, B). However, evident less autophagy was observed in IR and Thapsigargin treated cells compared with only IR treated cells. Autophagy and apoptosis related proteins such as P62, LC3II/I and (Cleaved) Caspase 3 were measured in cells of each group. It was confirmed that IR induce apparent autophagy and apoptosis of tumor cells by increasing LC3II/I and (Cleaved) Caspase 3 expression but decreasing P62 expression (Fig. 3C, D). Thapsigargin attenuated the effect of IR on apoptosis and autophagy mediated by P62, LC3II/I and (Cleaved) Caspase 3 expression. Further autophagy flow detection results displayed that IR induced increasing autophagy which was partially reversed by Calcium inhibitor (Fig. 3E, F).

#### Calcium-mediated TMEM147/SPHK1 regulates autophagy in tongue squamous cell carcinoma cells

The relation of calcium, TMEM147/SPHK1 and autophagy was explored to clarify the molecular mechanism of IR in our study. Results indicated that the expression of SPHK1 negatively correlated with TMEM147 from the protein expression detection in CAL27 and SAS cells transfection with TMEM147 over-expression plasmids (TMEM147-OE) (Fig. 4A, B). However, the effect of SPHK1 expression on TMEM147 expression was not as significant as that of TMEM147 expression on SPHK1 expression. It was suggested that TMEM147 may be upstream of SPHK1 (Fig. 4C, D). Immunoprecipitation

(See figure on next page.)

**Fig. 4** Calcium associates with TMEM147/SPHK1 to regulate autophagy in tongue squamous cell carcinoma cells. **A** The protein expression of TMEM147 and SPHK1 was assayed using western blotting in SAS and CAL27 cells transfected with TMEM147 overexpression (TM147-OE) vectors. **B** Relative protein expression of TMEM147 and SPHK1 was analyzed.  $n = 3$ ,  $**P < 0.01$ . **C** The protein expression of TMEM147 and SPHK1 was assayed using western blotting in SAS and CAL27 cells transfected with SPHK1 down expression (siSPHK1) vectors. **D** Relative protein expression of TMEM147 and SPHK1 was analyzed.  $n = 3$ ,  $**P < 0.01$ . **E** The protein interaction of TMEM147 and SPHK1 detected by immunoprecipitation. **F** Protein interaction of TMEM147 and SPHK1 was forecast from bioinformatics analysis. **G** Calcium levels image of CAL27 and SAS cells transfected with TM147-OE or siSPHK1 compared with negative control. **H** Autophagosomes were observed in CAL27 and SAS cells transfected with TM147-OE or siSPHK1 compared with negative control using transmission electron microscope. The red arrows indicate the autophagosomes with bilayer structure. The blue arrows indicate the decreasing autophagy

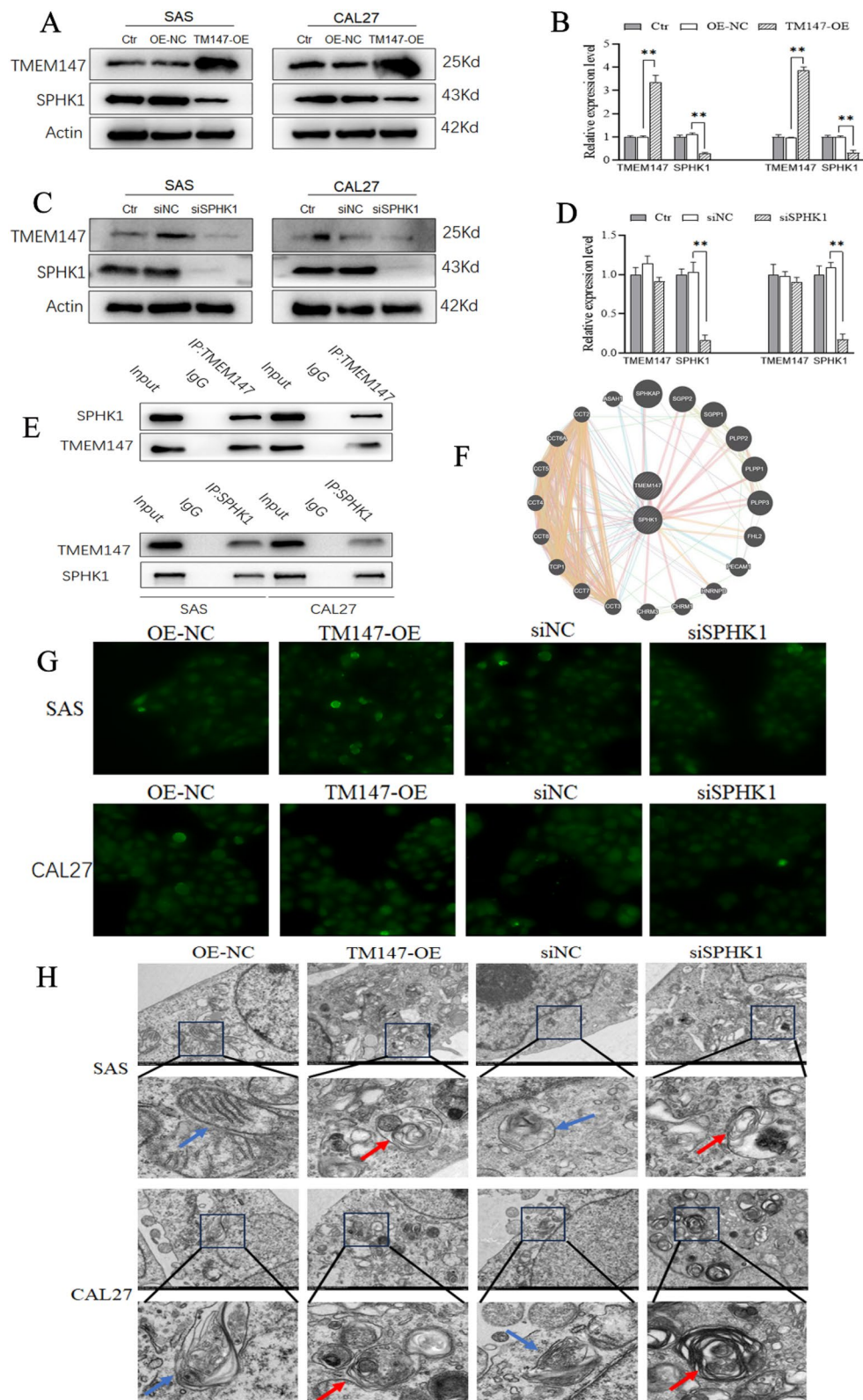


**Fig. 4** (See legend on previous page.)

and bioinformatics analysis results indicated that there was an interaction relationship between TMEM147 and SPHK1 (Fig. 4E, F). Result of calcium levels measurement showed that up-regulated TMEM147 expression (TMEM147-OE) as well as down-regulated SPHK1 expression (siSPHK1) has mild effect on calcium levels in CAL27 and SAS cells (Fig. 4G). Nevertheless, both TMEM147-OE and siSPHK1 induced significant autophagy in CAL27 and SAS cells (Fig. 4H). Our results suggested that calcium may mediate TMEM147/SPHK1 to regulate autophagy in tongue squamous cell carcinoma cells.

#### Calcium-mediated TMEM147/SPHK1 regulates autophagy to promote IR sensitivity in tongue squamous cell carcinoma in vitro

IR induced increasing calcium levels in both CAL27 and SAS cells with down-expression of TMEM147 (shTMEM147) and over-expression of SPHK1 (SPHK1-OE) (Fig. 5A, Fig. S1). Moreover, the calcium levels in CAL27 and SAS cells induced by IR were independent of TMEM147 and SPHK1 expression which may further suggest that calcium is upstream of TMEM147/SPHK1. However, shTMEM147 along with SPHK1-OE attenuated the inducing effect of IR on autophagy and it was suggested that TMEM147/SPHK1 could regulated autophagy in IR-treated tongue squamous cell carcinoma cells (Fig. 5B). Cell proliferation and apoptosis in CAL27 and SAS cells treated with IR was detected to explore the role of TMEM147/SPHK1 in tumor development. Results showed that shTMEM147 and SPHK1-OE partially reversed the effect of IR on cell proliferation inhibition (Fig. 5C, Fig. S2) and promoting apoptosis (Fig. 5D, Fig. S3, Fig. 5E, Fig. S4) in CAL27 and SAS cells which comparable to that of autophagy. The results of TMEM147/SPHK1 accompanied with (p)AMPK, (p)mTOR, P62, LC3II/I and (Cleaved) Caspase 3 expression in CAL27 (Fig. 5F, G) and SAS (Fig. 5H, I) cells demonstrated that the expression of TMEM147 as well as p-mTOR, p-AMPK, LC3II/I and (Cleaved) Caspase 3 was significantly increased while the expression of SPHK1 along with P62 was decreased in IR treated cells

transfected with negative control of shTMEM147 (shNC) and SPHK1-OE (OE-NC) compared with control cells without IR (Ctr) and shTMEM147 as well as SPHK1-OE transfection attenuated the effect of IR on the above proteins expression.

#### Calcium-mediated TMEM147/SPHK1 regulates autophagy to promote IR sensitivity in tongue squamous cell carcinoma in vivo

The role of TMEM147/SPHK1 in tumor growth was confirmed investigation. It was showed in Fig. 6A, B that tumor volume in shTMEM147 and SPHK1-OE, especially SPHK1-OE treated mice appeared to be increased significantly compared with those in shNC and OE-NC treated group. Cell apoptosis was detected in tumor tissue of mice. Results were showed in Fig. 6C, Fig. S5 that cell apoptosis was obviously increased in IR treated CAL27 and SAS cells compared with vehicle control group. Cell apoptosis rate in IR combined with Thapsigargin treated CAL27 and SAS cells exhibited less compared with only IR treated cells which confirmed that calcium play an important role in IR sensitivity in tongue squamous cell carcinoma. Compared with NC (sh or OE) group, both shTMEM147 and SPHK1-OE accompanied with IR-treated cells showed decreasing apoptosis rate which suggested that TMEM147/SPHK1 correlated with tumor IR sensitivity. The co-expression and location of TMEM147 and SPHK1 was then measured in tumor tissue of CAL27 and SAS cells. It was demonstrated that IR induced TMEM147 increasing accompanied with decreasing SPHK1 expression which was independent of Thapsigargin in tongue squamous cell carcinoma in mice (Fig. 6D). The expression of TMEM147/SPHK1 accompanied with (p)AMPK, (p)mTOR, P62, LC3II/I and (Cleaved) Caspase 3 in tumor tissue of mice was detected for further confirm TMEM147/SPHK1 related autophagy and apoptosis in tongue squamous cell carcinoma. The results in vivo were consistent with those in vitro that TMEM147, p-mTOR, p-AMPK, LC3II/I and (Cleaved) Caspase 3 was significantly increased while the expression of SPHK1 and P62 was decreased in tumor tissue

(See figure on next page.)

**Fig. 5** Calcium, TMEM147/SPHK1 and autophagy associate with IR sensitivity in tongue squamous cell carcinoma in vitro. CAL27 and SAS cells were infected with down expression TMEM147 (shTM147) or over expression SPHK1 (SPHK1-OE) lentivirus compared with negative control. **A** Calcium levels image of CAL27 and SAS cells in each group. **B** Autophagosomes were observed using transmission electron microscope. The red arrows indicate the autophagosomes with bilayer structure. The blue arrows indicate the decreasing autophagy. **C** Cell proliferation was accessed by clone formation. **D** Apoptosis was detected using flow cytometer. **E** DNA damage detection was mediated by  $\gamma$ H2AX assay. **F** Protein expression of (p) mTOR, (p) AMPK, TMEM147, SPHK1 P62, LC3II/I and (Cleaved) Caspase 3 in CAL27 cells was assayed by western blotting. **G** Relative protein expression was analyzed from blots of CAL27 cells. **H** Protein expression of (p) mTOR, (p) AMPK, TMEM147, SPHK1 P62, LC3II/I and (Cleaved) Caspase 3 in SAS cells was assayed by western blotting. **I** Relative protein expression was analyzed from blots of SAS cells. n = 3, \* P < 0.05, \*\*P < 0.01 compared with control(Ctr). ## P < 0.01 compared with siNC&IR. &&P < 0.01 compared with OE-NC&IR

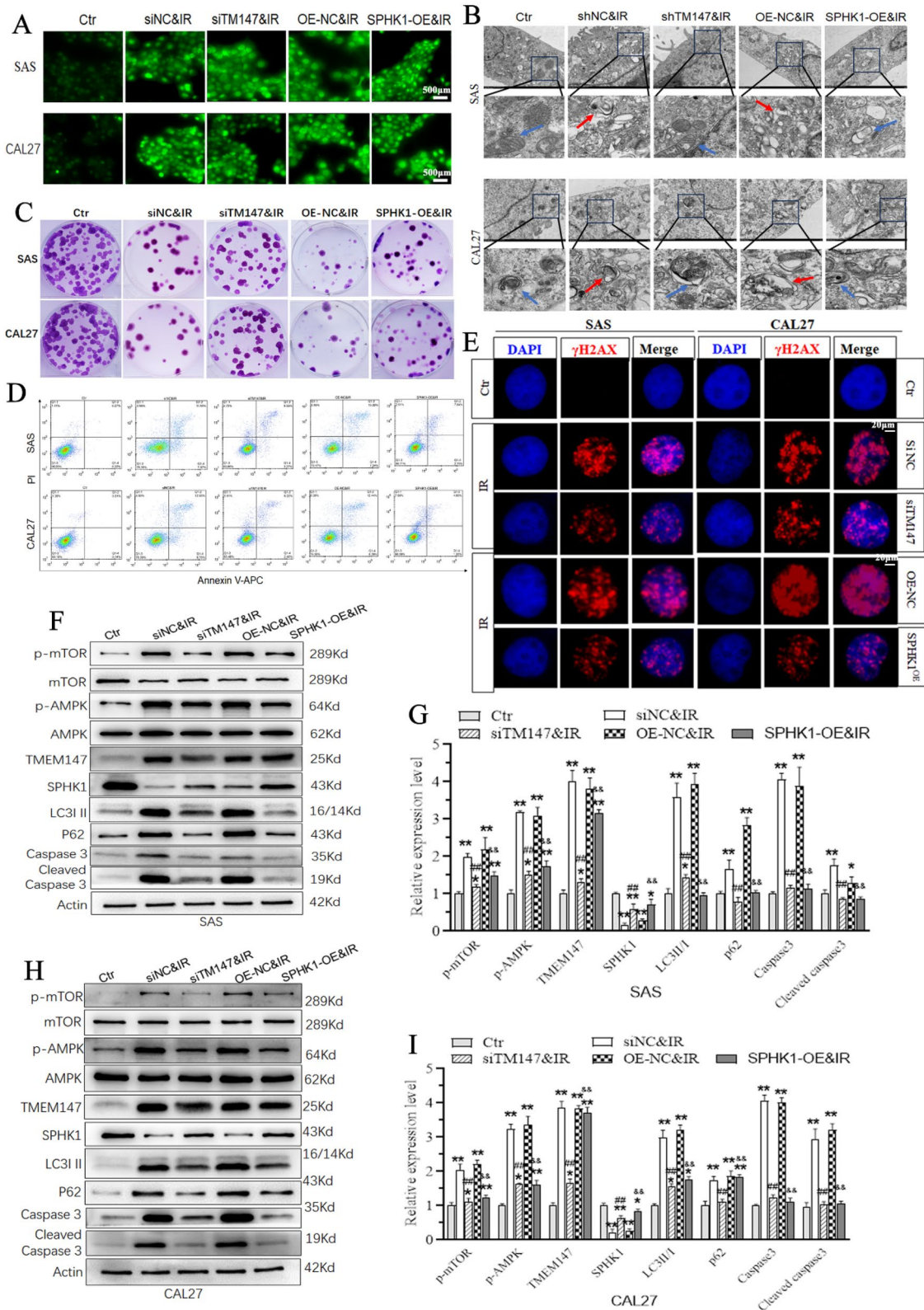


**Fig. 5** (See legend on previous page.)

of IR treated mice which was alleviated by Thapsigargin, shTMEM147 and SPHK1-OE combined treatment (Fig. 6E–H).

## Discussion

Radiotherapy sensitivity correlates with prognosis of patients with TSCC. Five differential proteins including TMEM147 and SPHK1 in IR treated TSCC cells compared with control ones were acquired according to the DIA quantitative proteomics and bioinformatics analysis in the present study. Previous study showed that TMEM147 expression was significantly increased in colon cancer compared with the control and associated with RNA polymerase and the purine metabolic pathways [21]. TMEM147 was also reported as a marker for overall survival prediction in osteosarcoma [22] and as a potential Sorafenib target to expedite cell cycle process and confer adverse prognosis in hepatocellular carcinoma [23]. As a novel biomarker for diagnosis and prognosis, TMEM147 correlates with immune infiltration and aggravates the progression by modulating cholesterol homeostasis, suppressing ferroptosis, and promoting the M2 polarization of tumor-associated macrophages in hepatocellular carcinoma [24–26]. However, the role of TMEM147 in TSCC remains unclear. SPHK1 is a pivotal prognostic gene in regulating tumor cell viability, migration, apoptosis, and anoikis along with over-expression in lung adenocarcinoma [27]. SPHK1 elevation facilitated cancer cell chemotherapy resistance [28]. Targeting SPHK1 may serve as a promising therapy for cancer resistance [29]. SPHK1 expression was up-regulated significantly in 70% oral squamous cell carcinoma tumors [30]. SPHK1 mediates head and neck squamous cell carcinoma invasion through sphingosine 1-phosphate receptor 1 [31]. A 15-gene signature including SPHK1 was independently associated with overall survival in non-distant metastatic TSCC [32]. TMEM147 and SPHK1 are then selected for further investigation in our study.

Results of the differential proteins involved TMEM147 and SPHK1 signal pathway enrichment analysis show that calcium signaling pathway is most significant. Calcium maybe involved in arterial IR [33]. Calcium-sensing receptor mediated balance of calcium has been

mentioned to associate with the development of various tumors, such as colorectal and breast tumors [34]. Therefore, the relation of calcium levels with IR treatment in TSCC was explored. Our results demonstrated that sensitivity of TSCC to IR was calcium dependent. The levels of calcium were increased when undergoing IR treatment which is consistent with the previous study that radiotherapy induced increasing intracellular calcium in esophageal squamous cell carcinoma cell lines [13].

Calcium participates in many cells processes involved cell signaling such as cell cycle, migration, invasion, apoptosis, autophagy, division, metabolism, differentiation, transcription, and others [35]. Autophagy and apoptosis as well as calcium level changes were investigated in our further study. It was demonstrated that IR treatment induced calcium intracellular accumulation positively correlated with increasing autophagy. Autophagy plays a dual role in resistance to chemotherapy and radiotherapy, metastasis and progression of tumors. Autophagy activation promotes malignant behavior of laryngeal carcinoma cells [36]. Autophagy showed carcinogenic function in breast tumor to cause drug resistance and radio-resistance so as to serve as an impediment towards effective therapy of patients [37]. Radio-resistance was mentioned to be promoted by triggering autophagy formation in oral squamous cell carcinoma [38]. The sensitivity of Tca8113 cells of TSCC to cisplatin and radiation could be improved by inhibiting autophagy using multiple pathways [39].

In another way, enhancing autophagy companies with promoting apoptosis in breast cancer cells [40] along with autophagy induction associated with anti-bladder cancer effects [41], results of which are consistent with our study that increasing autophagy, confirmed by autophagy and apoptosis-related markers such as P62, LC3 and mTOR/AMPK, accompanied with apoptosis positively in TSCC treated with IR. It was noting that IR induced increasing calcium levels correlated with autophagy and apoptosis of TSCC. This is probably due to IR-induced a large amount of calcium inflow and overload to contribute to mitochondrial damage and promote autophagy and apoptosis of tumors [42, 43].

(See figure on next page.)

**Fig. 6** Calcium, TMEM147/SPHK1 and autophagy associate with IR sensitivity in tongue squamous cell carcinoma in vivo. The mice were inoculated subcutaneously with CAL27 and SAS cells infected with (shTM147) or over expression SPHK1 (SPHK1-OE) lentivirus compared with negative control accompanied with IR and/or Thapsigargin treatment. **A** Images of tumors of mice were showed. **B** Tumor growth curves were plotted.  $n = 5$ , \* $P < 0.05$ . **C** Apoptosis was detected by Tunnel staining. **D** Co-expression and location of TMEM147 and SPHK1 was measured by immunofluorescence. **E** Protein expression of (p) mTOR, (p) AMPK, TMEM147, SPHK1 P62, LC3II/I and (Cleaved) Caspase 3 in tumors of mice inoculated subcutaneously with CAL27 cells was assayed by western blotting. **F** Relative protein expression was analyzed from blots of CAL27 cells. **G** Protein expression of (p) mTOR, (p) AMPK, TMEM147, SPHK1 P62, LC3II/I and (Cleaved) Caspase 3 in tumors of mice inoculated subcutaneously with SAS cells was assayed by western blotting. **H** Relative protein expression was analyzed from blots of SAS cells.  $n = 3$ , \* $P < 0.05$ , \*\* $P < 0.01$

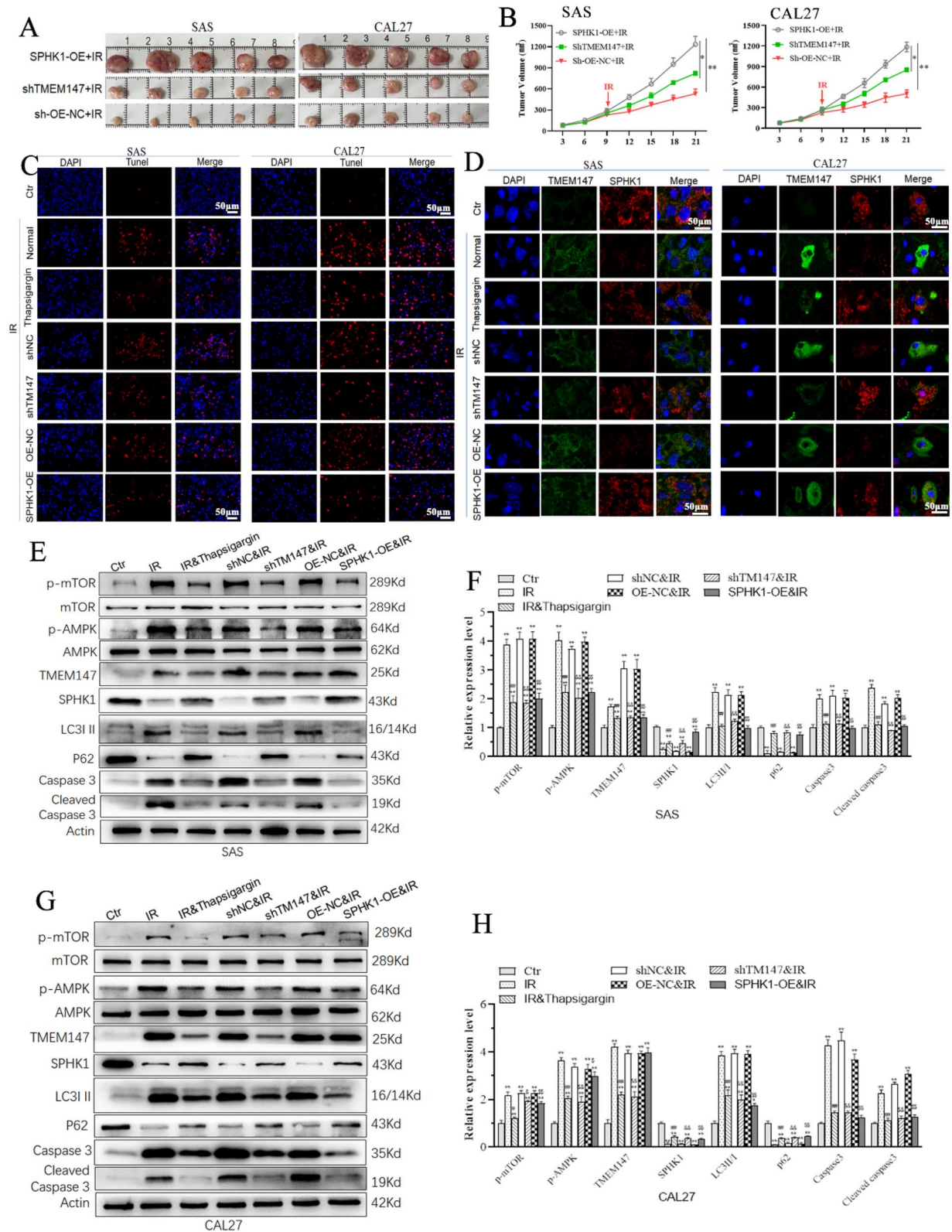


**Fig. 6** (See legend on previous page.)

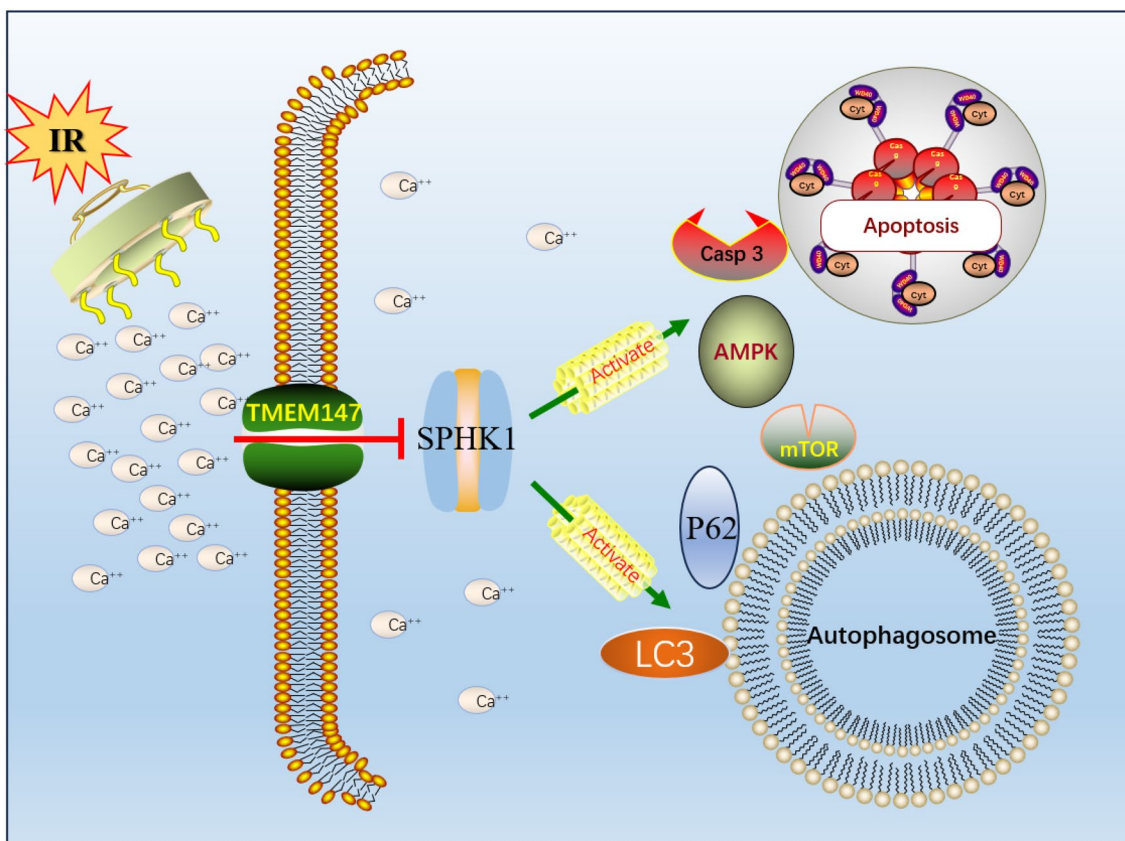


**Fig. 7** The role of TMEM147/SPHK1 in IR induced TSCC. Calcium mediated TMEM147/SPHK1 regulates autophagy to improve radiotherapy sensitivity in TSCC

Considering calcium signaling was involved in TMEM147 and SPHK1 which was related to autophagy, the regulatory relationship among calcium, TMEM147/SPHK1 and autophagy was further explored. Our results indicated that the increased levels of calcium induced by IR were independent of TMEM147 and SPHK1 expression. Otherwise, IR induced increasing calcium correlated with up-regulated TMEM147 along with down-regulated SPHK1 expression in TSCC to promote apoptosis and suppress tumor growth. It was suggested that calcium maybe the upstream regulatory factors of TMEM147/SPHK1. Analogously, the increase in autophagosomes was dependent of calcium levels as well as TMEM147 and SPHK1 expression but independent of calcium levels when down-expression of TMEM147 or over-expression of SPHK1. Results of the experimental and bioinformatics analysis of protein interactions show that TMEM147 could interact with SPHK1. Inhibition of SPHK1 activity alleviated mitochondrial oxidative damage in the renal tubular epithelial cells [44]. Calcium-mediated TMEM147/SPHK1 might be associated with radiotherapy sensitivity in head and

neck squamous cell carcinoma including TSCC. It was therefore proposed that IR-induced calcium overloading in TSCC promoted autophagy and apoptosis through TMEM147 suppressing SPHK1 activity. Our study will provide potential targets for improving radiotherapy sensitivity to improve prognosis of patients with TSCC .

## Conclusion

IR elevates calcium levels, up-regulates TMEM147, and down-regulates SPHK1 expression to promote autophagy and apoptosis in TSCC (Fig. 7).

## Supplementary Information

The online version contains supplementary material available at <https://doi.org/10.1186/s12967-024-05885-2>.

Supplementary Material 1

## Acknowledgements

Not Applicable.

## Author contributions

J.Z. and S.H. conceived the project and contributed to the experimental design. S.H. and X.L. conducted experiments., B.Y., T.Y., F.Y., X.Q., C.C., C.W. and

X.Y. helped to perform some experiments and data analysis. S.H. and X.L. wrote the draft of the manuscript. J.Z. supervised the project and revised the manuscript.

#### Funding

This study was supported by the National Nature Science Foundation of China (No. 82203964) and Science Talent Innovation Program of Shanghai Stomatological Hospital (No. SSH-2022-KJCX-B04), China.

#### Data availability

All data needed to evaluate the conclusions in the paper are present in the paper. Additional data related to this paper may be requested from the authors.

#### Declarations

##### Ethics approval and consent to participate

Not applicable.

##### Consent for publication

Not applicable.

##### Competing interests

The authors have declared that no competing interest exists.

Received: 14 August 2024 Accepted: 14 November 2024

Published online: 29 November 2024

#### References

- Bruballa R, Abuawad C, Boccalatte L, Larrañaga J. Tongue squamous cell carcinoma and bilateral kidney metastases. *Rev Fac Cien Med Univ Nac Cordoba*. 2021;78:184–7.
- Matsuo K, Akiba J, Kusukawa J, Yano H. Squamous cell carcinoma of the tongue: subtypes and morphological features affecting prognosis. *Am J Physiol Cell Physiol*. 2022;323:C1611–23.
- Mizuno K, Takeuchi M, Kikuchi M, Omori K, Kawakami K. Outcomes in patients diagnosed with tongue cancer before and after the age of 45 years. *Oral Oncol*. 2020;110:105010.
- da Silva Souto AC, Heimlich FV, de Oliveira LL, Bergmann A, Dias FL, Antunes HS, de Melo AC, Thuler LCS, Goldemberg DC. Epidemiology of tongue squamous cell carcinoma: a retrospective cohort study. *Oral Dis*. 2023;29:402–10.
- Lv X, Yu X. Signatures and prognostic values of related immune targets in tongue cancer. *Front Surg*. 2022;9:952389.
- Brock KK, Chen SR, Sheth RA, Siewerdsen JH. Imaging in interventional radiology: 2043 and beyond. *Radiology*. 2023;308:e230146.
- Suzuki-Shibata S, Yamamoto Y, Yoshida T, Mizoguchi N, Nonaka T, Kubota A, Narimatsu H, Miyagi Y, Kobayashi T, Kaneta T, Inoue T. Prognostic value of volumetric FDG PET/CT parameters in patients with oral tongue squamous cell carcinoma who were treated by superselective intra-arterial chemoradiotherapy. *Jpn J Radiol*. 2017;35:740–7.
- Turowski B, Zanella FE. Interventional neuroradiology of the head and neck. *Neuroimaging Clin N Am*. 2003;13:619–45.
- Arnold MJ, Keung JJ, McCarragher B. Interventional radiology: indications and best practices. *Am Fam Physician*. 2019;99:547–56.
- Montazersaheb S, Eftekhari A, Shafaroodi A, Tavakoli S, Jafari S, Baran A, Baran MF, Jafari S, Ahmadian E. Green-synthesized silver nanoparticles from peel extract of pumpkin as a potent radiosensitizer against triple-negative breast cancer (TNBC). *Cancer Nanotechnol* 2024, 15: 47.
- Baran MF, Keskin C, Baran A, Hatipoğlu A, Yıldıztekin M, Kūçūkaydın S, Kurt K, Hoşgören H, Sarker MMR, Sufianov A, et al. Green synthesis of silver nanoparticles from *Allium cepa* L. Peel extract, their antioxidant, antipathogenic, and anticholinesterase activity. *Molecules*. 2023; 10.3390/molecules28052310.
- Xu J, Yıldıztekin M, Han D, Keskin C, Baran A, Baran MF, Eftekhari A, Ava CA, Kandemir S, Cebe DB, et al. Biosynthesis, characterization, and investigation of antimicrobial and cytotoxic activities of silver nanoparticles using solanum tuberosum peel aqueous extract. *Heliyon*. 2023;9:e19061.
- Wang C, Li TK, Zeng CH, Yang J, Wang Y, Lu J, Zhu GY, Guo JH. Inhibition of endoplasmic reticulum stress-mediated autophagy enhances the anticancer effect of iodine-125 seed radiation on esophageal squamous cell carcinoma. *Radiat Res*. 2020;194:236–45.
- Al-Jamaei AH, de Visscher J, Subramanyam VR, Forouzanfar T, Sminia P, Doulabi BZ, Helder MN. WEE1 kinase inhibitor MK-1775 sensitizes oral tongue squamous cell carcinoma cells to radiation irrespective of TP53 status. *Oral Dis*. 2023;29:2640–9.
- Abdollahi E, Mozdarani H. Role of the circ-HIPK3, circ-PVT1, miR-25, and miR-149 in response of breast cancer cells to ionizing radiation. *Cell J*. 2023;25:688–95.
- Wang J, Hu T, Wang Q, Chen R, Xie Y, Chang H, Cheng J. Repression of the AURKA-CXCL5 axis induces autophagic cell death and promotes radio-sensitivity in non-small-cell lung cancer. *Cancer Lett*. 2021;509:89–104.
- Young KH, Baird JR, Savage T, Cottam B, Friedman D, Bambina S, Messenheimer DJ, Fox B, Newell P, Bahjat KS, et al. Optimizing timing of immunotherapy improves control of tumors by hypofractionated radiation therapy. *PLoS ONE*. 2016;11:e0157164.
- Hu S, Zhu L, Song Y, Zhao X, Chen Q, Pan Y, Zhang J, Bai Y, Zhang H, Shao C. Radiation-induced abscopal reproductive effect is driven by TNF- $\alpha$ /p38 MAPK/Rac1 axis in sertoli cells. *Theranostics*. 2021;11:5742–58.
- Cheratta AR, Thayyullathil F, Hawley SA, Ross FA, Atrih A, Lamont DJ, Pallichankandy S, Subburayan K, Alakkal A, Rezgui R, et al. Caspase cleavage and nuclear retention of the energy sensor AMPK- $\alpha$ 1 during apoptosis. *Cell Rep*. 2022;39:110761.
- Cao J, Mai H, Chen Y, Yuan R, Fang E, Liu M, Fu C. Ketamine promotes LPS-induced pulmonary autophagy and reduces apoptosis through the AMPK/mTOR pathway. *Contrast Med Mol Imag*. 2022;2022:8713701.
- Feng Y, Li Y, Li L, Wang X, Chen Z. Identification of specific modules and significant genes associated with colon cancer by weighted gene co-expression network analysis. *Mol Med Rep*. 2019;20:693–700.
- Du Y, Zeng X, Yu W, Xie W. A transmembrane protein family gene signature for overall survival prediction in osteosarcoma. *Front Genet*. 2022;13:937300.
- Ma W, Zhang X, Lu J, Lv S, Zhang Z, Ma H, Chen Q, Cao W, Zhang X. Transmembrane protein 147, as a potential Sorafenib target, could expedite cell cycle process and confer adverse prognosis in hepatocellular carcinoma. *Mol Carcinog*. 2023;62:1295–311.
- Fan WJ, Zhou MX, Wang DD, Jiang XX, Ding H. TMEM147 is a novel biomarker for diagnosis and prognosis of hepatocellular carcinoma. *Genet Mol Biol*. 2023;46:e20220323.
- Huang J, Pan H, Sun J, Wu J, Xuan Q, Wang J, Ke S, Lu S, Li Z, Feng Z, et al. TMEM147 aggravates the progression of HCC by modulating cholesterol homeostasis, suppressing ferroptosis, and promoting the M2 polarization of tumor-associated macrophages. *J Exp Clin Cancer Res*. 2023;42:286.
- Cheng S, Li J, Xu M, Bao Q, Wu J, Sun P, Han B. TMEM147 correlates with immune infiltration and serve as a potential prognostic biomarker in hepatocellular carcinoma. *Anal Cell Pathol (Amst)*. 2023;2023:4413049.
- He S, Xiao X, Ma C, Liu Y, Lin Q, Qian W, Cao C, Ren S, Chen J, Mi Y, Shen D. Identification and immunological characteristics of anoikis-associated molecular clusters in lung adenocarcinoma. *Exp Cell Res*. 2024;438:114037.
- Liu D, Liu L, Li H, Huang Z, Wang Y. Sphingosine kinase 1 counteracts chemosensitivity and immune evasion in diffuse large B cell lymphoma cells via the PI3K/AKT/PD-L1 axis. *Int Immunopharmacol*. 2024;143:113361.
- Alkafaas SS, Elsalahaty MI, Ismail DF, Radwan MA, Elkafas SS, Loutfy SA, Elshazli RM, Baazaoui N, Ahmed AE, Hafez W, et al. The emerging roles of sphingosine 1-phosphate and SphK1 in cancer resistance: a promising therapeutic target. *Cancer Cell Int*. 2024;24:89.
- Vishwakarma S, Agarwal R, Goel SK, Panday RK, Singh R, Sukumaran R, Khare S, Kumar A. Altered expression of sphingosine-1-phosphate metabolizing enzymes in oral cancer correlate with clinicopathological attributes. *Cancer Invest*. 2017;35:139–41.
- Tamashiro PM, Furuya H, Shimizu Y, Kawamori T. Sphingosine kinase 1 mediates head & neck squamous cell carcinoma invasion through sphingosine 1-phosphate receptor 1. *Cancer Cell Int*. 2014;14:76.

32. Liu M, Tong L, Liang B, Song X, Xie L, Peng H, Huang D. A 15-gene signature and prognostic nomogram for predicting overall survival in non-distant metastatic oral tongue squamous cell carcinoma. *Front Oncol.* 2021;11:587548.
33. Zhao K, Patel N, Kulkarni K, Gross JS, Taslakian B. Essentials of insulinoma localization with selective arterial calcium stimulation and hepatic venous sampling. *J Clin Med.* 2020;10.3390/jcm9103091.
34. Basic-Pavlek I, Dumic-Cule I, Kovacevic L, Milosevic M, Delimar P, Korsal L, Marusic Z, Prutki M. Calcium-sensing receptor expression in breast cancer. *Int J Mol Sci.* 2023;10.3390/ijms241411678.
35. Pratt SJP, Hernández-Ochoa E, Martin SS. Calcium signaling: breast cancer's approach to manipulation of cellular circuitry. *Biophys Rev.* 2020;12:1343–59.
36. Guo F, Wen W, Mi Z, Long C, Shi Q, Yang M, Zhao J, Ma R. NRSN2 promotes the malignant behavior of HPV-transfected laryngeal carcinoma cells through AMPK/ULK1 pathway mediated autophagy activation. *Cancer Biol Ther.* 2024;25:2334463.
37. Hashemi M, Paskeh MDA, Orouei S, Abbasi P, Khorrami R, Dehghanpour A, Esmaili N, Ghahremanzade A, Zandieh MA, Peymani M, et al. Towards dual function of autophagy in breast cancer: a potent regulator of tumor progression and therapy response. *Biomed Pharmacother.* 2023;161:114546.
38. Yuan TZ, Lin HY, Kuei CH, Lin CH, Lee HH, Lee HL, Lu HW, Su CY, Chiu HW, Lin YF. NEDD8 promotes radioresistance via triggering autophagy formation and serves as a novel prognostic marker in oral squamous cell carcinoma. *Cancer Cell Int.* 2023;23:41.
39. Ma B, Hu Y, Zhu J, Zheng Z, Ye J. Research on the role of cellular autophagy in the sensitivity of human tongue cancer cells to radiotherapy and chemotherapy. *J Stomatol Oral Maxillofac Surg.* 2023;124:101430.
40. Jiang G, Zhou X, Hu Y, Tan X, Wang D, Yang L, Zhang Q, Liu S. The antipsychotic drug pimozide promotes apoptosis through the RAF/ERK pathway and enhances autophagy in breast cancer cells. *Cancer Biol Ther.* 2024;25:2302413.
41. Luo S, Huang X, Li S, Chen Y, Zhang X, Zeng X. Homogeneous polyporus polysaccharide exerts anti-bladder cancer effects via autophagy induction. *Pharm Biol.* 2024;62:214–21.
42. Liu L, Chen Y, Ye L, Yu L, Kang Y, Mou X, Cai Y. NIR-II absorbed dithienopyrrole-benzobisthiadiazole based nanosystems for autophagy inhibition and calcium overload enhanced photothermal therapy. *Small.* 2024; 10.1002/smll.202309891 .
43. de la Harpe A, Beukes N, Frost C. Mitochondrial calcium overload contributes to cannabinoid-induced paraptosis in hormone-responsive breast cancer cells. *Cell Prolif* 2024: 10.1111/cpr.13650.
44. Hou Y, Tan E, Shi H, Ren X, Wan X, Wu W, Chen Y, Niu H, Zhu G, Li J, et al. Mitochondrial oxidative damage reprograms lipid metabolism of renal tubular epithelial cells in the diabetic kidney. *Cell Mol Life Sci.* 2024;81:23.

## Publisher's note

Springer Nature remains neutral with regard to jurisdictional claims in published maps and institutional affiliations.